# CRISPR-engineered human brown-like adipocytes prevent diet-induced obesity and ameliorate metabolic syndrome in mice

**Chih-Hao Wang**[1,2], **Morten Lundh**[1,3,4], **Accalia Fu**[5,6], **Rókus Kriszt**[7,8], **Tian Lian Huang**[1], **Matthew D. Lynes**[1], **Luiz O. Leiria**[9,10], **Farnaz Shamsi**[1], **Justin Darcy**[1], **Bennett P. Greenwood**[11], **Niven R. Narain**[11], **Vladimir Tolstikov**[11], **Kyle L. Smith**[12], **Brice Emanuelli**[3], **Young-Tae Chang**[13,14], **Susan Hagen**[12], **Nika N. Danial**[5], **Michael A. Kiebish**[11], **Yu-Hua Tseng**[1,15,*]

[1]Section on Integrative Physiology and Metabolism, Joslin Diabetes Center, Harvard Medical School, Boston, MA 02215, USA

[2]Graduate Institute of Biomedical Sciences, China Medical University, Taichung 40402, Taiwan

[3]The Novo Nordisk Foundation Center for Basic Metabolic Research, University of Copenhagen, DK-2200, Denmark

[4]Gubra Aps, Hørsholm, DK-2970, Denmark

[5]Department of Cancer Biology, Dana-Farber Cancer Institute, Harvard Medical School, Boston, MA 02215, USA.

[6]Department of Cell Biology, Harvard Medical School, Boston, MA 02215, USA.

[7]Department of Biomedical Engineering, National University of Singapore, Singapore, 117583

[8]Graduate School for Integrative Sciences and Engineering (NGS), National University of Singapore, Singapore, 119077

[9]Department of Pharmacology, Ribeirao Preto Medical School, University of São Paulo, Ribeirão Preto, 14049-900, Brazil

[10]Center of Research of Inflammatory Diseases, Ribeirao Preto Medical School, University of São Paulo, Ribeirão Preto, 14049-900, Brazil

[11]BERG, Framingham, MA 01701, USA

[12]Department of Surgery, Beth Israel Deaconess Medical Center, Boston, MA 02215, USA

[13]Center for Self-assembly and Complexity, Institute for Basic Science (IBS), Pohang, Republic of Korea, 34126

[14]Department of Chemistry, Pohang University of Science and Technology (POSTECH), Pohang, Republic of Korea, 37673

[15]Harvard Stem Cell Institute, Harvard University, Cambridge, MA 02138, USA

## Abstract

Brown and brown-like beige/brite adipocytes dissipate energy and have been proposed as therapeutic targets to combat metabolic disorders. However, the therapeutic effects of cell-based therapy in humans remain unclear. Here, we created human brown-like (HUMBLE) cells by engineering human white preadipocytes using CRISPR/Cas9-SAM-gRNA to activate endogenous uncoupling protein 1 expression. Obese mice that received HUMBLE cell transplants showed a sustained improvement in glucose tolerance and insulin sensitivity, as well as increased energy expenditure. Mechanistically, increased arginine/nitric oxide (NO) metabolism in HUMBLE adipocytes promoted the production of NO that was carried by S-nitrosothiols and nitrite in red blood cells to activate endogenous brown fat and improved glucose homeostasis in recipient animals. Taken together, these data demonstrate the utility of using CRISPR/Cas9 technology to engineer human white adipocytes to display brown fat-like phenotypes and may open up cell-based therapeutic opportunities to combat obesity and diabetes.

## One Sentence Summary:

Human white adipocytes engineered to express UCP1 activate endogenous BAT and protect against diet-induced obesity when transplanted into mice.

## INTRODUCTION

Obesity and metabolic syndrome are rapidly increasing worldwide, leading to high morbidity and mortality. Developing preventive and therapeutic strategies for obesity and its complications is of great importance to the healthcare community (1, 2). In mammals, both brown adipose tissue (BAT) and white adipose tissue (WAT) contribute to systemic energy homeostasis; however, their anatomy, morphology, and functions are quite different. WAT is the main site for storing excess fuel containing unilocular lipid droplets, whereas BAT is specific for energy dissipation and possesses multilocular lipid droplets (3).

Activation of BAT increases energy expenditure, and its activity is inversely correlated with body mass index and fat mass, making BAT an appealing target for anti-obesity therapies (4-7). BAT generates heat in response to cold exposure due to its unique expression of uncoupling protein 1 (*UCP1*) that dissipates energy by uncoupling the proton motive force from ATP production. Although *UCP1* expression is restricted to BAT under basal conditions, prolonged cold exposure or β3-adrenergic stimulation can not only increase UCP1-mediated thermogenic capacity in BAT, but can also activate the recruitment of brown-like beige (also termed brite) adipocytes in WAT that express *UCP1* to produce heat in a process called browning. In adult humans, WAT is distributed throughout the body and located on the superficial fat pads; however, BAT presents itself in small regions of deep fat

pads such as the cervical, supraclavicular, and paravertebral regions (8). Considering its abundance and location, WAT is more easily reachable and manipulatable. Induced browning of WAT may hold great potential for preventing or treating obesity and obesity-related metabolic disorders.

Although some UCP1-independent thermogenic mechanisms have been identified in beige/brite adipocytes (9, 10), there is no doubt that the activation of UCP1-mediated thermogenesis is an efficient way to waste excess energy and consume fuels for metabolic health benefits (11). Mice that ectopically express *UCP1* in skeletal muscle (12, 13) and adipose tissue (14, 15) are protected from diet-induced obesity. Pigs lack a functional *UCP1* gene, and ectopic expression of *UCP1* in white fat promotes lipolysis and cold tolerance in these animals (16). These studies clearly demonstrate the anti-obesogenic effect of ectopically overexpressed *UCP1* in animals; however, it is unclear whether these effects can be recapitulated in humans by activating the endogenous *UCP1* locus.

Cell-based therapies offer the potential to contribute to unmet patient needs and treat diseases that existing pharmaceuticals cannot adequately address. One potential benefit of a cell-based approach compared to strategies based around single molecules may be a more comprehensive and persistent therapeutic effect. Autologous cell therapy is a preferred therapeutic intervention where cells are taken from an individual and administered into the same individual to minimize immune rejection. Autologous cell-based therapies have been an active area of research, and are moving towards successful commercial development and patient access due to breakthroughs in delivery systems and genome engineering methods such as CRISPR (17, 18).

The CRISPR/Cas9 system provides a powerful means for genome editing in mammalian cells (19) and several new tools have been developed based on CRISPR/Cas9 to allow targeted inhibition or activation of gene expression. In CRISPR activation techniques, a nuclease-deactivated Cas9 (dCas9) is fused with transactivation domains and directed by a single guide (sg) RNA targeting a specific promoter where this synthetic transcriptional complex can activate expression of the endogenous gene (20). CRISPR activation systems have been applied to drive differentiation, transdifferentiation, and reprogramming of various mouse and human cell types (21-25). This technique has been used to activate browning genes in mouse white preadipocytes (26). However, the effects of CRISPR-engineered cells on whole body metabolism and their therapeutic potential to battle obesity and obesity-related disorders have not been tested.

One of the advanced versions of CRISPR activation is the Synergistic Activation Mediator (SAM) system wherein dCas9 is combined with a fusion protein consisting of two transcriptional activation domains from nuclear factor kappa-light-chain-enhancer of activated B cells (NF-kB) and heat-shock factor 1 (HSF1) to synergistically boost transcription (20). Here, we used the CRISPR-SAM system in human white preadipocytes (27) to activate *UCP1* gene expression. In addition to characterizing these CRISPR-engineered human cells, we also demonstrated the therapeutic potential of these cells by treating obesity and metabolic disorders in mice.

# RESULTS

### Endogenous activation of UCP1 by CRISPR-SAM triggers brown-like phenotypes in human white adipocytes

We have previously established paired immortalized human brown and white preadipocytes (27-29). Here we used these cells to generate human brown fat-like adipocytes from white adipose precursor cells and compared the resulting cells to bona fide human brown adipocytes derived from the same individual. To this end, we adapted the CRISPR-SAM system (20) to increase endogenous *UCP1* expression in human white preadipocytes. We designed 4 different gRNAs (labelled A-D) targeting around 50-150 bp upstream of the human *UCP1* gene, and stably expressed vectors encoding dCas9 fused with VP64, a fusing protein containing the MS2 bacteriophage coat protein, the NFκB trans-activating subunit p65, and the activation domain of HSF1 (MS2-p65-HSF1) (Fig. 1A). Lentiviral transduction of the CRISPR-SAM system combined with gRNAs A-D into human white preadipocytes derived from two subjects. gRNA-A resulted in approximately 6000-fold increase in *UCP1* mRNA and about a 20-fold increase in UCP1 protein (Fig. 1, B and C). Notably, *UCP1* expression in white preadipocytes transduced with sgRNA-A was comparable to that detected in differentiated human brown adipocytes from the same individual. Several loci were predicted as potential alternate targets of sgRNA-A; however, we detected no off-target changes in the expression of genes downstream of these sites (fig. S1A). These findings demonstrate combining CRISPR-SAM and sgRNAs targeting *UCP1* allows engineering of human white preadipocytes into huMan brown-like (HUMBLE) cells by turning on endogenous *UCP1* expression.

HUMBLE preadipocytes can be induced to differentiate into lipid-laden UCP1-positive adipocytes (Fig. 1, D to F). Compared to the original human white adipocytes lacking sgRNA (hereafter called white control cells or adipocytes), HUMBLE cells maintained high *UCP1* expression after adipogenic differentiation. However, the *UCP1* expression in HUMBLE cells was slightly lower than in differentiated brown adipocytes from the same individual (brown control cells; Fig. 1, E and F). HUMBLE cells displayed elevated *GLUT1* mRNA compared with the white control adipocytes, whereas the expression of BAT selective markers iodothyronine deiodinase 2 (*DIO2*) and beta-3 adrenergic receptor (*ADRB3*) were not changed (Fig. 1G). Expression of genes involved in mitochondrial biogenesis and activities, such as *PGC1a*, *NRF1,* and *CPT1b*, was increased by 2~3-fold in HUMBLE cells (Fig. 1G), which led to increased mitochondrial activity (Fig. 1H) and mtDNA content (fig. S1B) comparable with brown control adipocytes. Compared to white control adipocytes, HUMBLE cells exhibited a more elongated and connected mitochondrial network that resembled the mitochondrial morphology of brown control adipocytes (Fig. 1I and fig. S1C).

In addition to possessing the molecular and structural features of brown control adipocytes, HUMBLE cells also acquired brown fat-like functional phenotypes. Compared to white control cells, HUMBLE adipocytes had increased glucose uptake (fig. S1D), basal respiratory rate, proton leak, and forskolin (FSK)-dependent oxygen consumption rate (OCR) while utilizing glucose as a substrate (fig. S1E). They also had a higher capacity for

fatty acid-dependent OCR than did the white control cells (Fig. 1J, and fig. S1F), whereas fatty acid uptake was not altered (fig. S1G). Using thermosensitive fluorescent ERthermAC dye (29) we directly measured heat production in cultured cells and found that HUMBLE cells generated more heat compared to white control cells in response to forskolin (Fig. 1K). Treating cells with GDP to inhibit UCP1 normalized fatty acid-dependent OCR and heat production (Fig. 1, J and K), suggesting that the increased metabolism and thermogenesis in HUMBLE cells was UCP1-dependent. These findings suggest that HUMBLE cells are thermogenically competent in utilizing glucose or fatty acids as a fuel source.

## UCP1 activation promotes mitochondrial biogenesis and function via AMPK

Searching for a potential link between the elevated *UCP1* expression and the observed increase in mitochondrial biogenesis and function, we found that both intracellular AMP concentrations and AMPK phosphorylation were elevated in HUMBLE cells compared to white control cells (fig. S1, H and I), indicating increased proton uncoupling action by *UCP1* overexpression. Inhibition of AMPK activity by knockdown of AMPKα (siAMPKα) abolished the increased mitochondrial OCR in HUMBLE cells (fig. S1J). AMPK has been shown to regulate mitochondrial biogenesis via induction of *PGC1α* expression (30), and indeed, expression of *PGC1α* and the mitochondrial transcription factor *NRF1* was also elevated in HUMBLE cells (Fig. 1G). These data suggest that the high degree of uncoupled respiration in HUMBLE cells leads to AMPK activation, which in turn upregulates mitochondrial biogenesis and function to adapt to the increased energy dissipation in HUMBLE cells.

## HUMBLE cells reconstitute functional adipocytes in mice

Transplantation of genetically engineered (31) or pharmacologically induced (32), beige/brite cells improves metabolism homeostasis in mice. To determine the metabolic impact of HUMBLE cells in vivo, white control, HUMBLE, and brown control preadipocytes were mixed with Matrigel and transplanted into the thoracic-sternum region of immune-compromised nude mice (Fig. 2A). All of these cells also expressed a luciferase reporter driven by the human *UCP1* promoter (27), which allowed longitudinal monitoring of *UCP1* expression in the transplanted human cells in vivo. At 2 weeks after transplantation, HUMBLE cells showed the highest of luciferase signal among the three transplanted cell lines (Fig. 2B). By 4 weeks, we detected substantial *UCP1* expression in both brown control and HUMBLE cells (Fig. 2C), suggesting that at this point the brown control preadipocytes had differentiated into mature adipocytes with upregulation of *UCP1* expression. Indeed, when we examined the transplanted human cells histologically, it was apparent that the implanted preadipocytes had differentiated in vivo into fat-like tissues with adipocytes containing unilocular or multilocular lipid droplets (Fig. 2D) that expressed the mature adipocyte marker *aP2* (Fig. 2E). In addition, the transplanted tissues became vascularized and innervated as shown by positive staining for mouse CD31 and tyrosine hydroxylase, respectively (Fig. 2D). We detected human adiponectin in the mouse sera (Fig. 2F), indicating that the transplants were functional and could act as endocrine tissues to secrete adipokines or other factors into circulation. Notably, although HUMBLE transplants displayed a unilocular lipid droplet phenotype similar to tissues derived from the parental white control cells, they expressed high UCP1 protein and mRNA expression comparable to

the multilocular brown control fat cell transplants (Fig. 2, D and E). Furthermore, mitochondria from the HUMBLE transplants had a more well-defined and compact cristae structure similar to the mitochondria in the brown control transplants (Fig. 2G). Together, these data demonstrate that the transplanted preadipocytes could reconstitute fat tissues in vivo that recapitulated the phenotypes of these cells in vitro.

### HUMBLE cells facilitate glucose metabolism and thermogenesis in mice

Next, to investigate whether HUMBLE cells can prevent mice from metabolic disorders in diet-induced obesity, we monitored the metabolic phenotypes of recipient mice that were fed with a 45% high fat diet (HFD) for 2 weeks prior to transplantation, and continued the same diet for 4 weeks after transplantation (Fig. 3A). Mice receiving HUMBLE and brown control fat cells gained less weight than mice receiving white control cells (Fig. 3B). Mice with HUMBLE or brown control cell transplants also displayed approximately 30% to 35% improvements in glucose tolerance and insulin sensitivity compared with mice receiving white control cells (Fig. 3, C and D). There was no statistically significant change in serum insulin, however circulating triglyceride (TG) concentrations were decreased in the HUMBLE and brown control cell groups compared to mice receiving the white control cells (fig. S2, A and B). Mice transplanted with HUMBLE or brown control cells also consumed more oxygen and generated more heat than white control cell recipients in the dark cycle, whereas there was no difference in food intake (Fig. 3E, and fig. S2, C to F). HUMBLE or brown control fat cell transplantation allowed mice to maintain a higher core body temperature upon cold exposure compared to mice receiving white control cell transplantation (Fig. 3F). The improved metabolic phenotypes of HUMBLE cell transplantation were observed in 6 independent cohorts; and there were 6-8 mice per cohort. It is also important to note that white control cell transplantation had no effect on body weight, glucose tolerance, oxygen consumption, or heat production compared to mice transplanted with Matrigel alone (fig. S2, G to J), suggesting that transplantation of the white control cells did not have any negative effect on metabolism.

To further validate the metabolic effects of HUMBLE cells in vitro and in vivo, we generated an additional line of HUMBLE cells using white preadipocytes isolated from another individual (A38) and the same CRISPR-SAM system (Fig. 3, G and H). Consistent with the aforementioned protective effects in cells derived from donor A41, HUMBLE cells created from donor A38 also showed high thermogenic potential in vitro (Fig. 3I), and when transplanted in vivo using the same protocol, improved glucose tolerance, insulin sensitivity, and energy metabolism compared to their parental white control preadipocytes. Furthermore, all phenotypes were comparable to brown control preadipocytes derived from the same donor (Fig. 3, J to L, and fig. S3). These results indicate that the CRISPR-based HUMBLE cell strategy is applicable to different human subjects. Finally, all the beneficial effects of a HUMBLE or brown control preadipocyte transplant can be recapitulated by transplanting mature HUMBLE or brown control adipocytes that were differentiated in vitro prior to implantation (fig. S4).

### HUMBLE cell transplantation displays long-term metabolic benefits in mice

To test how long the beneficial effects on metabolism could be sustained, we monitored the HFD-fed mice transplanted with different cell types for up to 12 weeks (Fig. 4A). Mice receiving HUMBLE or brown control cells stayed leaner compared to the white control cell recipients throughout the entire 12 weeks (Fig. 4B). Whereas the glucose tolerance of mice receiving white control cells deteriorated over time, mice receiving HUMBLE or brown control cells showed improved glucose tolerance even at 12 weeks post-transplantation (Fig. 4, C to F). Moreover, *UCP1* reporter activity was still detectable at 12 weeks after transplantation, indicating that the transplanted cells remained viable (Fig. 4, G to I).

### HUMBLE cell transplantation improves metabolism in diet-induced obese mice

To examine the potential of using HUMBLE cells for treating obesity, we transplanted cells into nude mice with diet-induced obesity (DIO) (Fig. 5A). DIO mice transplanted with HUMBLE or brown control cells gained less weight than mice transplanted with white control cells (Fig. 5B), which corresponded with great improvements in glucose tolerance and insulin sensitivity as well as lower circulating insulin concentrations at 4 weeks after transplantation (Fig. 5, C to F). Liver lipid contents were decreased in mice transplanted with HUMBLE or brown control cells compared to mice transplanted with white control cells, with a corresponding decrease in the size of lipid droplets in endogenous BAT and subcutaneous WAT (scWAT) (Fig. 5G). Taken together, these data demonstrate that HUMBLE cell transplantation may be a potential anti-obesity therapeutic strategy.

### HUMBLE cell transplant activates endogenous murine BAT in vivo

To determine which tissues contributed to the increased glucose disposal in mice that received HUMBLE or brown control cells, we measured glucose uptake in vivo. Mice receiving HUMBLE or brown control cells cleared the glucose radiotracer from circulation more rapidly than mice with white control cell transplantation (Fig. 6A). This was attributable to increased glucose uptake into the endogenous murine BAT rather than enhanced glucose uptake by the transplanted cells (Fig. 6B, and fig. S5A). The endogenous murine BAT from mice receiving HUMBLE or brown control cells had smaller lipid droplets and more highly expressed genes encoding BAT selective markers such as *Ucp1*, *Prdm16*, *Pgc1α*, and *Dio2*, as well as genes involved glucose or fatty acid metabolism including *Glut1*, *Pparγ*, *Ppara*, *Cpt1b,* and *Cpt2* compared to BAT from mice receiving white control cells (Fig. 6, C and D). There was no change in glucose uptake (Fig. 6, B, and fig. S5A) or expression of any of the aforementioned genes in endogenous scWAT or skeletal muscle (fig. S5, B and C). Functionally, cold challenge resulted in higher surface temperatures near the endogenous BAT in mice receiving HUMBLE or brown control cells than in mice transplanted with white control cells (Fig. 6E), suggesting an activation of adaptive thermogenesis of recipient mice. These data indicate that HUMBLE and brown control cells could activate endogenous BAT.

### HUMBLE cells promote function of human and mouse brown adipocytes in vitro

To model the crosstalk between HUMBLE cells and murine BAT, as well as potential communication between HUMBLE cells and human BAT, we co-cultured HUMBLE cells

with in vitro-differentiated mouse or human brown adipocytes in a transwell culture system (fig. S5D).Basal and insulin-stimulated glucose uptake into murine brown adipocytes co-cultured with white control cells were both increased by co-culture with HUMBLE cells compared to co-culture with white control adipocytes (Fig. 6F). Increased glucose uptake was also observed in human brown cells (fig. S5E). In addition, murine brown cells treated with conditioned medium from HUMBLE cells (fig. S5F) displayed higher mitochondrial respiration and greater thermogenic capacity than when treated with the white control cell-conditioned medium (Fig. 6, G and H). These findings provide evidence that HUMBLE cells improve systemic glucose homeostasis by activating endogenous BAT via secreted factors.

## HUMBLE cells display elevated arginine and nitric oxide metabolism

Murine BAT transplantation has been shown improvement of whole-body metabolism via its endocrine function (33-36), for which IL6 (35) or IGF1 (36) secreted from BAT transplants has been demonstrated as a mediator. However, the abundance of these two proteins in secreted media of HUMBLE cells and in the serum of mice receiving HUMBLE transplants displayed no difference compared to the white control cell group (fig. S6, A and B). To identify potential factors that could mediate communication between HUMBLE cells and endogenous murine BAT, we performed a metabolomics analysis in the conditioned medium from differentiated white control, HUMBLE, and brown control adipocytes. Principal component analysis and heatmap analysis showed that metabolite profiles from HUMBLE and brown control cells shared a high degree of similarity to the metabolite profile from the brown control group (Fig. 7, A to C). Further pathway analysis of the differentially produced metabolites between HUMBLE or brown control vs. white control cells led us to focus on arginine metabolism (Fig. 7, B and C).

Notably, the abundance of three major metabolites involved in arginine metabolism, including arginine itself, were increased in the media of HUMBLE and brown control cells compared to that of white control cells (Fig. 7D). Arginine and citrulline were also elevated in cellular extracts from HUMBLE cells compared to white control cells (Fig. 7E). This was accompanied by increased mRNA expression and activity of endothelial nitric oxide synthase (eNOS) (Fig. 7, F and G), an enzyme that converts arginine to citrulline and produces nitric oxide (NO). Last, total nitric oxide (nitrite and nitrate) concentrations were increased by 2-fold in the media from HUMBLE and brown control cells compared to white control cells (Fig. 7H). To address if the increase in NO metabolism resulted from UCP1-mediated uncoupling effects in HUMBLE cells, we aimed to inhibit AMPK, which was activated by the proton-uncoupling action of *UCP1* overexpression (fig. S1, H and I). Increased *eNOS* expression and NO concentrations were abolished in HUMBLE cells with *AMPK* knockdown (fig. S6, C and D), suggesting that the increased uncoupling effect due to *UCP1* overexpression promotes NO metabolism via AMPK activation.

In terms of arginine utilization, brown control cells displayed increased both NO and urea pathways compared to white control cells, whereas HUMBLE cells appeared to activate only the NO pathway. The expression and activity of arginase 2 (ARG2) and secreted urea concentrations were elevated in brown control cells but not in HUMBLE cells compared to white control cells (Fig. 7F, and fig. S6, E to G). Integrating gene expression with

metabolomics data indicated that HUMBLE cells have enhanced arginine and NO metabolism (see pathways in Fig. 7I, and fig. S6, H to J). To test if NO produced from HUMBLE cells could play a role in activating mouse or human brown adipocytes, we co-cultured human and murine brown adipocytes with *eNOS* knockout (*eNOS* KO) HUMBLE cells which had diminished NO production (fig. S6K). Loss of eNOS and NO production abrogated the effect of HUMBLE cells on promoting glucose uptake into human or murine brown cells (Fig. 7J). These data indicate that NO produced from arginine metabolism in HUMBLE cells can activate brown adipocytes in vitro.

### HUMBLE cells activate endogenous BAT through red blood cell-mediated NO delivery

Because HUMBLE cell transplantation did not affect circulating abundances of arginine, citrulline, or ornithine (fig. S7A), and based on our in vitro findings and the reported regulatory role of NO in BAT (37), we hypothesized that the transplanted HUMBLE or brown control cells could secrete NO to promote endogenous murine BAT activation in vivo. Although NO often exerts its effects in a paracrine or autocrine fashion, red blood cells (RBCs) have been reported to reversibly bind, transport, and release NO to other tissues (38, 39). Thus, we hypothesized that RBCs could serve as a mediator to transport NO to endogenous murine BAT. Indeed, RBCs isolated from mice receiving HUMBLE or brown control cells contained higher concentrations of total nitrite and nitrate compared to RBCs isolated from white control cell recipient mice (Fig. 8A). Given that NO bioactivity in RBCs can also be carried by S-nitrosothiols (SNO) that mediate NO cardiovascular effects (40, 41), we measured the amount of S-nitrosylation in RBCs to determine NO bioavailability in mice. RBCs from mice receiving HUMBLE or brown control cells displayed increased S-nitrosylation measured by biotin switch assay (Fig. 8B) and by gel Cy5-labeling (Fig. 8C, and fig. S7B). The endogenous murine BAT from these mice had elevated total nitrite and nitrate and S-nitrosylation with a corresponding increase in cyclic guanosine monophosphate (cGMP), a signaling molecule downstream of NO, compared with BAT from mice receiving white control cells (Fig. 8, D and E, and fig. S7C). In an in vitro co-culture system, we found that murine brown adipocytes displayed elevated concentrations of total nitrite and nitrate after co-culture with RBCs collected from mice receiving HUMBLE cells (Fig. 8F), upregulated expression of *Ucp1* and *Dio2* (fig. S7D), and showed increased glucose uptake (fig. S7E) compared to those co-cultured with RBCs from mice receiving white control cells. These findings suggest that NO from HUMBLE cells carried by RBCs promotes glucose uptake and thermogenic program in endogenous BAT.

Along with no effect on gene activation (fig. S5, A and B), total nitrite and nitrate concentrations were not changed in scWAT or skeletal muscle (fig. S7F). In accordance with the known regulatory role of NO on vascular function (42) both HUMBLE and brown control transplants elevated blood flow within the endogenous murine BAT region in comparison to white control cell transplantation, whereas blood flow in the scWAT region was unaltered (fig. S7G). These results suggest that RBCs deliver NO to BAT in a tissue-targeted manner.

**Inhibition of NO production abolishes HUMBLE cell-mediated metabolic benefits**

To determine whether NO plays an essential role in mediating the effects of HUMBLE cells in vivo, we generated HUMBLE cells with an *eNOS* knockout (KO). After transiently transfecting wild-type Cas9 and *eNOS* gene-targeted sgRNA into white preadipocytes to knockout *eNOS*, we generated HUMBLE cells with *eNOS* KO by introducing the CRISPR-SAM system with UCP1 sgRNA-A into *eNOS* KO cells by Thus, we hypothesized that RBCs could serve as a mediator to transport NO to endogenous murine BAT. Indeed, RBCs isolated from mice receiving HUMBLE or brownlentivirus. After transplanting white control, HUMBLE, or HUMBLE cells with *eNOS* knockout into nude mice (Fig. 8G), loss of eNOS in HUMBLE transplants diminished their effect on body weight, glucose tolerance, thermal regulation, energy metabolism, and activation of endogenous murine BAT (Fig. 8, H to J, and fig. S8, A to E) associated with the abrogation of increased S-nitrosylation in RBCs (fig. S8, F and G). Moreover, transplanting *eNOS*-overexpressing white control cells (fig. S9, A and B) showed comparable systemic metabolic benefits with HUMBLE transplantation (fig. S9, C to K). Taken together, these data reveal the mechanistic requirement of eNOS activation in HUMBLE cells to direct higher NO concentrations in endogenous BAT transported by RBCs.

## Discussion

In the present study, we engineered human white preadipocytes using the CRISPR-SAM system to activate the endogenous *UCP1* gene and drive a brown-like phenotype. By taking advantage of paired human white and brown pre-adipocyte cell lines (27) we were able to compare the engineered HUMBLE cells and their isogenic parental white control cells to bona fide brown control cells from the same individual, providing an accurate phenotypic comparison. Our data demonstrate the preclinical therapeutic potential of the CRISPR-engineered HUMBLE cells in prevention and treatment of obesity. Transplantation of HUMBLE cells highly improved glucose homeostasis in mice, which was mediated, at least in part, by SNO/nitrite-facilitated activation of endogenous murine BAT (fig. S9L).

In our studies, transplanted human preadipocytes differentiated into adipocytes in situ and, more importantly, developed the vascularization and innervation needed for adipocyte function in an obese mouse model. Additionally, the transplanted cells survived in vivo for at least 12 weeks, such that the beneficial effects of these cells on whole-body glucose homeostasis in recipient mice were sustained. Our in vivo results utilizing both preventive and treatment models suggest that HUMBLE cell-based therapy could potentially be used for combating metabolic disorders caused by high-caloric diets.

We found that the major contribution of glucose uptake was from the endogenous BAT, instead of from the transplant itself, even though HUMBLE and brown control cells displayed a high capacity for thermogenesis as well as glucose and fatty acid uptake in vitro. Although these data may seem contradictory, they point out fundamental differences between in vitro and in vivo systems, which involve intercellular communications within and outside the tissues of interest. Compared to endogenous tissues, effects from the transplant itself may be mild due to the relatively smaller size of transplanted cells. Although there was vascularization in the human transplants, they were not as fully vascularized as endogenous

tissues for the circulation to deliver large amount of blood glucose to the transplanted tissue for uptake and utilization. This may limit the glucose uptake ability in the transplant. However, it is important to point out that the vascularization in transplants is sufficient to secrete human adiponectin into circulation, and to communicate with the endogenous BAT by RBC-mediated NO delivery.

The metabolic effect of HUMBLE transplantation appears to be mediated via RBC-mediated delivery of nitric oxide in the form of SNO/nitrite shuttling to the endogenous murine BAT. Although it has been shown that the overexpression of *UCP1* does not affect endogenous BAT (14), other studies have demonstrated potential roles of transplanted mouse BAT (34-36) or human beige adipocytes (32) in communicating with endogenous tissues, including BAT, to improve systemic glucose homeostasis in the recipient mouse. We note that there are certain methodological differences among these studies. It has been shown that using a transgene to overexpress *UCP1* in endogenous adipose tissues, which does not involve cell or tissue transplantation (14, 15). It is worth noting that transplantation studies, including ours, identify different secreted factors in activating endogenous tissues and modulating systemic glucose utilization. This difference may result from the different species of transplants (mouse or human), different cell types (whole tissue, beige cells, brown-like cells), and different transplantation sites (visceral cavity, subcutaneous tissue). These dissimilarities may drive differential signals that contribute to the distinct molecular mechanisms underlying those studies.

By integrating gene expression and metabolomics data, we have shown that HUMBLE cells have higher arginine and NO metabolism than parental white control cells. In our model, HUMBLE cell transplantation induced NO-mediated activation of BAT, leading to increased expression of thermogenic genes, glucose uptake, and blood flow. The effect of NO carried by RBCs in a form of S-nitrosothiols/nitrite target to endogenous BAT exclusively, which may reflect the high degree of vascularization of this tissue to allow high exposure to RBCs. It has also been demonstrated that hypoxic and acidic environment can trigger release of NO from S-nitrosothiol hemoglobin (SNO-Hb) (43-45) or from nitrite by nitrite reductase (39). Given that BAT is a highly oxygen-consuming tissue with high amounts of lactate, this could produce a hypoxic and acidic microenvironment, facilitating NO release from RBCs (46, 47) in BAT.

NO has emerged as a central regulator of energy metabolism and body composition that acts mainly by modulating the oxidative capacity and insulin sensitivity of adipose tissue (37). With obesity, insulin resistance, and cardiovascular disorders, NO bioactivity is decreased in the circulation of both animals (48) and humans (49). Inhibition of systemic NO synthesis, or *eNOS* knockout in mice, results in increased circulating triglyceride concentrations and body fat mass with no change in food intake (50, 51). Increasing NO output by dietary arginine supplementation (52) or inorganic nitrate (53) has an anti-obesogenic effect and improves insulin sensitivity. Mechanistically, nitrates increase the expression of thermogenic genes in BAT and induce the expression of brown adipocyte–specific genes in WAT, substantially increasing oxygen consumption and fatty acid β-oxidation in adipocytes (54). NO induces mitochondrial biogenesis by activating PGC-1α (50) and inhibiting

mitochondrial fission (55), which may underlie the increased mitochondrial biogenesis and elongated mitochondria in HUMBLE cells.

Our model demonstrates that NO has a unique effect on BAT. Cold and norepinephrine can induce NO production via activation of the β3-adrenergic receptor, which results in vasodilation and increased blood flow in BAT (56). Recently, metabolomics analysis has shown that the arginine metabolism pathway is activated in BAT after acute cold exposure (57). Ablation of soluble guanylyl cyclase (sGC), a downstream effector of NO signaling, severely impairs BAT function; pharmacological sGC stimulation protects against DIO and induces weight loss by enhancing differentiation of brown adipocytes (58). Our HUMBLE cell-based therapy may provide an alternative strategy to activate BAT by increasing NO bioactivity by, in part, increasinged eNOS activity in HUMBLE cells.

Although several clinical studies have demonstrated that cold exposure is an effective way of activating BAT (4, 59, 60), therapeutic cold exposure is uncomfortable for humans. Moreover, sympathomimetics drugs can effectively activate BAT but possess unwanted cardiovascular side effects (5, 61, 62). In our study, transplantation of HUMBLE cells, which activates the endogenous BAT, does not cause any side effects on blood pressure or heart rate, and can sustainably improve metabolism for a prolonged period. This study provides a potential strategy to combat obesity and metabolic syndrome by using CRISPR engineered human brown-like cells combined with an autologous cell transfer based therapy.

There are limitations to this work. We used immunocompromised nude mice as the recipients for HUMBLE cell transplantation to avoid immune rejection of the human cell transplants. However, the deficiency of specific immune cells and cytokines in the immunocompromised mice is likely to affect the results and interpretation of the metabolic assessments. In addition, all the experiments were conducted in one animal facility. Thus, facility-specific environmental factors, such as ambient temperature, diet, housing condition, and microbiota, may influence the observed phenotypes. Last, we used immortalized preadipocytes derived from two human subjects to generate the HUMBLE cells. The application of such an approach in primary cells derived from a larger number of individuals warrants future investigation.

## MATERIALS AND METHODS

### Study design

The main objective of the study was to create human brown-like adipocytes from white adipocytes by CRISPR engineering and to determine the effects of these CRISPR-engineered human brown-like (HUMBLE) adipocytes on whole-body glucose metabolism and thermogenesis in obese mice. To avoid immune rejection of human cell transplantation, we transplanted cells into nude mice and selected the thoracic-sternum region for transplantation due to less endogenous fat there, enhanced observation, and easy retrieval of the transplants (27). We designed different protocols to evaluate the therapeutic potential of HUMBLE cells. In the prevention cohort, we transplanted cells into mice 2 weeks after HFD feeding. In the treatment cohort, we performed transplantation in mice 12 weeks after HFD feeding. We also monitored the change in metabolism after transplantation up to 12 weeks to

evaluate long-term effects in the prevention cohort. The study was extended by generating human brown-like adipocytes from white adipocytes isolated from a second individual to prove the concept and increase the generalizability of HUMBLE cell therapy. Metabolomics analysis using LC-MS/MS technology was conducted to identify the putative metabolic pathway involved in the improvement of glucose metabolism in the mice. For in vivo experiments, age-matched mice were randomly allocated to different groups, but the experimenters were not blinded. Blinding was only performed for calculating mitochondrial cristae scores. Animal studies were performed according to procedures approved by the Joslin Diabetes Center Institutional Animal Care and Use Committee (IACUC). All experiments were repeated at least three times. Only mice in poor health identified by a veterinarian (for example unreasonable weight loss, low activity, or severe damage from fighting) were excluded from data analysis. We excluded 3 mice in the treatment cohort before cell transplantation and 2 mice in the long-term monitoring cohort. We did not exclude any outliers in our data analysis.

### Statistical analysis

No statistical method was used to predetermine sample size. All statistics were calculated using Microsoft Excel and GraphPad Prism. Data were tested for a normal (Gaussian) distribution using Shapiro-Wilk normality test. Two-tailed Student's t test was performed for all 2 group comparisons. One-Way ANOVA followed by a Tukey's post-hoc test was performed when comparing more than 3 groups. Significance was defined as $*P < 0.05$, $**P < 0.01$, $***P < 0.001$.

## Supplementary Material

Refer to Web version on PubMed Central for supplementary material.

## Acknowledgments:

## REFERENCES AND NOTES

1. Kopelman PG, Obesity as a medical problem. Nature 404, 635–643 (2000). [PubMed: 10766250]

2. Cornier MA, Dabelea D, Hernandez TL, Lindstrom RC, Steig AJ, Stob NR, Van Pelt RE, Wang H, Eckel RH, The metabolic syndrome. Endocr. Rev 29, 777–822 (2008). [PubMed: 18971485]

3. Leitner BP, Huang S, Brychta RJ, Duckworth CJ, Baskin AS, McGehee S, Tal I, Dieckmann W, Gupta G, Kolodny GM, Pacak K, Herscovitch P, Cypess AM, Chen KY, Mapping of human brown adipose tissue in lean and obese young men. Proc. Natl. Acad. Sci. U. S. A 114, 8649–8654 (2017). [PubMed: 28739898]

4. Blondin DP, Labbe SM, Phoenix S, Guerin B, Turcotte EE, Richard D, Carpentier AC, Haman F, Contributions of white and brown adipose tissues and skeletal muscles to acute cold-induced metabolic responses in healthy men. J. Physiol 593, 701–714 (2015). [PubMed: 25384777]

5. Cypess AM, Chen YC, Sze C, Wang K, English J, Chan O, Holman AR, Tal I, Palmer MR, Kolodny GM, Kahn CR, Cold but not sympathomimetics activates human brown adipose tissue in vivo. Proc. Natl. Acad. Sci. U. S. A 109, 10001–10005 (2012). [PubMed: 22665804]

6. Cypess AM, Lehman S, Williams G, Tal I, Rodman D, Goldfine AB, Kuo FC, Palmer EL, Tseng YH, Doria A, Kolodny GM, Kahn CR, Identification and importance of brown adipose tissue in adult humans. New England Journal of Medicine 360, 1509–1517 (2009). [PubMed: 19357406]

7. van Marken Lichtenbelt WD, Vanhommerig JW, Smulders NM, Drossaerts JM, Kemerink GJ, Bouvy ND, Schrauwen P, Teule GJ, Cold-activated brown adipose tissue in healthy men. New Engl. J. Med 360, 1500–1508 (2009). [PubMed: 19357405]

8. Ouellet V, Labbe SM, Blondin DP, Phoenix S, Guerin B, Haman F, Turcotte EE, Richard D, Carpentier AC, Brown adipose tissue oxidative metabolism contributes to energy expenditure during acute cold exposure in humans. J. Clin. Invest 122, 545–552 (2012). [PubMed: 22269323]

9. Kazak L, Chouchani ET, Jedrychowski MP, Erickson BK, Shinoda K, Cohen P, Vetrivelan R, Lu GZ, Laznik-Bogoslavski D, Hasenfuss SC, Kajimura S, Gygi SP, Spiegelman BM, A creatine-driven substrate cycle enhances energy expenditure and thermogenesis in beige fat. Cell 163, 643–655 (2015). [PubMed: 26496606]

10. Ikeda K, Kang Q, Yoneshiro T, Camporez JP, Maki H, Homma M, Shinoda K, Chen Y, Lu X, Maretich P, Tajima K, Ajuwon KM, Soga T, Kajimura S, UCP1-independent signaling involving SERCA2b-mediated calcium cycling regulates beige fat thermogenesis and systemic glucose homeostasis. Nat. Med 23, 1454–1465 (2017). [PubMed: 29131158]

11. Ost M, Keipert S, Klaus S, Targeted mitochondrial uncoupling beyond UCP1 - The fine line between death and metabolic health. Biochimie 134, 77–85 (2017). [PubMed: 27916644]

12. Li B, Nolte LA, Ju JS, Han DH, Coleman T, Holloszy JO, Semenkovich CF, Skeletal muscle respiratory uncoupling prevents diet-induced obesity and insulin resistance in mice. Nature Medicine 6, 1115–1120 (2000).

13. Neschen S, Katterle Y, Richter J, Augustin R, Scherneck S, Mirhashemi F, Schurmann A, Joost HG, Klaus S, Uncoupling protein 1 expression in murine skeletal muscle increases AMPK activation, glucose turnover, and insulin sensitivity in vivo. Physiological Genomics 33, 333–340 (2008). [PubMed: 18349383]

14. Kopecky J, Clarke G, Enerback S, Spiegelman B, Kozak LP, Expression of the mitochondrial uncoupling protein gene from the aP2 gene promoter prevents genetic obesity. Journal of Clinical Investigation 96, 2914–2923 (1995). [PubMed: 8675663]

15. Kopecky J, Hodny Z, Rossmeisl M, Syrovy I, Kozak LP, Reduction of dietary obesity in aP2-Ucp transgenic mice: physiology and adipose tissue distribution. American Journal of Physiology 270, E768–775 (1996). [PubMed: 8967464]

16. Zheng Q, Lin J, Huang J, Zhang H, Zhang R, Zhang X, Cao C, Hambly C, Qin G, Yao J, Song R, Jia Q, Wang X, Li Y, Zhang N, Piao Z, Ye R, Speakman JR, Wang H, Zhou Q, Wang Y, Jin W, Zhao J, Reconstitution of UCP1 using CRISPR/Cas9 in the white adipose tissue of pigs decreases fat deposition and improves thermogenic capacity. Proc Natl Acad Sci U S A 114, E9474–E9482 (2017). [PubMed: 29078316]

17. De Luca M, Aiuti A, Cossu G, Parmar M, Pellegrini G, Robey PG, Advances in stem cell research and therapeutic development. Nat Cell Biol 21, 801–811 (2019). [PubMed: 31209293]

18. Yin H, Xue W, Anderson DG, CRISPR-Cas: a tool for cancer research and therapeutics. Nat Rev Clin Oncol 16, 281–295 (2019). [PubMed: 30664678]

19. Cong L, Ran FA, Cox D, Lin S, Barretto R, Habib N, Hsu PD, Wu X, Jiang W, Marraffini LA, Zhang F, Multiplex genome engineering using CRISPR/Cas systems. Science 339, 819–823 (2013). [PubMed: 23287718]

20. Konermann S, Brigham MD, Trevino AE, Joung J, Abudayyeh OO, Barcena C, Hsu PD, Habib N, Gootenberg JS, Nishimasu H, Nureki O, Zhang F, Genome-scale transcriptional activation by an engineered CRISPR-Cas9 complex. Nature 517, 583–588 (2015). [PubMed: 25494202]

21. Kearns NA, Genga RM, Enuameh MS, Garber M, Wolfe SA, Maehr R, Cas9 effector-mediated regulation of transcription and differentiation in human pluripotent stem cells. Development 141, 219–223 (2014). [PubMed: 24346702]

22. Wei S, Zou Q, Lai S, Zhang Q, Li L, Yan Q, Zhou X, Zhong H, Lai L, Conversion of embryonic stem cells into extraembryonic lineages by CRISPR-mediated activators. Sci. Rep 6, 19648 (2016). [PubMed: 26782778]

23. Liu P, Chen M, Liu Y, Qi LS, Ding S, CRISPR-Based Chromatin Remodeling of the Endogenous Oct4 or Sox2 Locus Enables Reprogramming to Pluripotency. Cell Stem Cell 22, 252–261 e254 (2018). [PubMed: 29358044]

24. Black JB, Adler AF, Wang HG, D'Ippolito AM, Hutchinson HA, Reddy TE, Pitt GS, Leong KW, Gersbach CA, Targeted Epigenetic Remodeling of Endogenous Loci by CRISPR/Cas9-Based Transcriptional Activators Directly Converts Fibroblasts to Neuronal Cells. Cell Stem Cell 19, 406–414 (2016). [PubMed: 27524438]

25. Weltner J, Balboa D, Katayama S, Bespalov M, Krjutskov K, Jouhilahti EM, Trokovic R, Kere J, Otonkoski T, Human pluripotent reprogramming with CRISPR activators. Nat. Commun 9, 2643 (2018). [PubMed: 29980666]

26. Lundh M, Plucinska K, Isidor MS, Petersen PSS, Emanuelli B, Bidirectional manipulation of gene expression in adipocytes using CRISPRa and siRNA. Mol Metab 6, 1313–1320 (2017). [PubMed: 29031730]

27. Xue R, Lynes MD, Dreyfuss JM, Shamsi F, Schulz TJ, Zhang H, Huang TL, Townsend KL, Li Y, Takahashi H, Weiner LS, White AP, Lynes MS, Rubin LL, Goodyear LJ, Cypess AM, Tseng YH, Clonal analyses and gene profiling identify genetic biomarkers of the thermogenic potential of human brown and white preadipocytes. Nat. Med 21, 760–768 (2015). [PubMed: 26076036]

28. Townsend KL, Tseng YH, Brown fat fuel utilization and thermogenesis. Trends Endocrinol. Metab 25, 168–177 (2014). [PubMed: 24389130]

29. Kriszt R, Arai S, Itoh H, Lee MH, Goralczyk AG, Ang XM, Cypess AM, White AP, Shamsi F, Xue R, Lee JY, Lee SC, Hou Y, Kitaguchi T, Sudhaharan T, Ishiwata S, Lane EB, Chang YT, Tseng YH, Suzuki M, Raghunath M, Optical visualisation of thermogenesis in stimulated single-cell brown adipocytes. Sci. Rep 7, 1383 (2017). [PubMed: 28469146]

30. Herzig S, Shaw RJ, AMPK: guardian of metabolism and mitochondrial homeostasis. Nat. Rev. Mol. Cell Biol 19, 121–135 (2018). [PubMed: 28974774]

31. Kajimura S, Seale P, Kubota K, Lunsford E, Frangioni JV, Gygi SP, Spiegelman BM, Initiation of myoblast to brown fat switch by a PRDM16-C/EBP-beta transcriptional complex. Nature 460, 1154–1158 (2009). [PubMed: 19641492]

32. Min SY, Kady J, Nam M, Rojas-Rodriguez R, Berkenwald A, Kim JH, Noh HL, Kim JK, Cooper MP, Fitzgibbons T, Brehm MA, Corvera S, Human 'brite/beige' adipocytes develop from capillary networks, and their implantation improves metabolic homeostasis in mice. Nat Med 22, 312–318 (2016). [PubMed: 26808348]

33. Wang GX, Zhao XY, Meng ZX, Kern M, Dietrich A, Chen Z, Cozacov Z, Zhou D, Okunade AL, Su X, Li S, Bluher M, Lin JD, The brown fat-enriched secreted factor Nrg4 preserves metabolic homeostasis through attenuation of hepatic lipogenesis. Nat Med 20, 1436–1443 (2014). [PubMed: 25401691]

34. Liu X, Wang S, You Y, Meng M, Zheng Z, Dong M, Lin J, Zhao Q, Zhang C, Yuan X, Hu T, Liu L, Huang Y, Zhang L, Wang D, Zhan J, Jong Lee H, Speakman JR, Jin W, Brown Adipose Tissue Transplantation Reverses Obesity in Ob/Ob Mice. Endocrinology 156, 2461–2469 (2015). [PubMed: 25830704]

35. Stanford KI, Middelbeek RJ, Townsend KL, An D, Nygaard EB, Hitchcox KM, Markan KR, Nakano K, Hirshman MF, Tseng YH, Goodyear LJ, Brown adipose tissue regulates glucose homeostasis and insulin sensitivity. J. Clin. Invest 123, 215–223 (2013). [PubMed: 23221344]

36. Gunawardana SC, Piston DW, Reversal of type 1 diabetes in mice by brown adipose tissue transplant. Diabetes 61, 674–682 (2012). [PubMed: 22315305]

37. Jankovic A, Korac A, Buzadzic B, Stancic A, Otasevic V, Ferdinandy P, Daiber A, Korac B, Targeting the NO/superoxide ratio in adipose tissue: relevance to obesity and diabetes management. Br. J. Pharmacol 174, 1570–1590 (2017). [PubMed: 27079449]

38. Owusu BY, Stapley R, Patel RP, Nitric oxide formation versus scavenging: the red blood cell balancing act. J. Physiol 590, 4993–5000 (2012). [PubMed: 22687616]

39. Dejam A, Hunter CJ, Pelletier MM, Hsu LL, Machado RF, Shiva S, Power GG, Kelm M, Gladwin MT, Schechter AN, Erythrocytes are the major intravascular storage sites of nitrite in human blood. Blood 106, 734–739 (2005). [PubMed: 15774613]

40. Zhang R, Hess DT, Qian Z, Hausladen A, Fonseca F, Chaube R, Reynolds JD, Stamler JS, Hemoglobin betaCys93 is essential for cardiovascular function and integrated response to hypoxia. Proc. Natl. Acad. Sci. U. S. A 112, 6425–6430 (2015). [PubMed: 25810253]

41. Zhang R, Hess DT, Reynolds JD, Stamler JS, Hemoglobin S-nitrosylation plays an essential role in cardioprotection. J. Clin. Invest 126, 4654–4658 (2016). [PubMed: 27841756]

42. Lundberg JO, Gladwin MT, Weitzberg E, Strategies to increase nitric oxide signalling in cardiovascular disease. Nat. Rev. Drug Discov 14, 623–641 (2015). [PubMed: 26265312]

43. Lane P, Gross S, Hemoglobin as a chariot for NO bioactivity. Nat. Med 8, 657–658 (2002). [PubMed: 12091894]

44. Diesen DL, Hess DT, Stamler JS, Hypoxic vasodilation by red blood cells: evidence for an s-nitrosothiol-based signal. Circ. Res 103, 545–553 (2008). [PubMed: 18658051]

45. Doctor A, Platt R, Sheram ML, Eischeid A, McMahon T, Maxey T, Doherty J, Axelrod M, Kline J, Gurka M, Gow A, Gaston B, Hemoglobin conformation couples erythrocyte S-nitrosothiol content to O2 gradients. Proc. Natl. Acad. Sci. U. S. A 102, 5709–5714 (2005). [PubMed: 15824313]

46. Khanna A, Branca RT, Detecting brown adipose tissue activity with BOLD MRI in mice. Magn. Reson. Med 68, 1285–1290 (2012). [PubMed: 22231619]

47. Reber J, Willershauser M, Karlas A, Paul-Yuan K, Diot G, Franz D, Fromme T, Ovsepian SV, Beziere N, Dubikovskaya E, Karampinos DC, Holzapfel C, Hauner H, Klingenspor M, Ntziachristos V, Non-invasive Measurement of Brown Fat Metabolism Based on Optoacoustic Imaging of Hemoglobin Gradients. Cell Metab. 27, 689–701 e684 (2018). [PubMed: 29514074]

48. Kim F, Pham M, Maloney E, Rizzo NO, Morton GJ, Wisse BE, Kirk EA, Chait A, Schwartz MW, Vascular inflammation, insulin resistance, and reduced nitric oxide production precede the onset of peripheral insulin resistance. Atertio. Thromb. Vasc. Biol 28, 1982–1988 (2008).

49. Gruber HJ, Mayer C, Mangge H, Fauler G, Grandits N, Wilders-Truschnig M, Obesity reduces the bioavailability of nitric oxide in juveniles. Int. J. Obes. (Lond.) 32, 826–831 (2008). [PubMed: 18197180]

50. Nisoli E, Clementi E, Paolucci C, Cozzi V, Tonello C, Sciorati C, Bracale R, Valerio A, Francolini M, Moncada S, Carruba MO, Mitochondrial biogenesis in mammals: the role of endogenous nitric oxide. Science 299, 896–899 (2003). [PubMed: 12574632]

51. Khedara A, Goto T, Morishima M, Kayashita J, Kato N, Elevated body fat in rats by the dietary nitric oxide synthase inhibitor, L-N omega nitroarginine. Biosci., Biotechnol., Biochem 63, 698–702 (1999). [PubMed: 10361682]

52. Jobgen W, Meininger CJ, Jobgen SC, Li P, Lee MJ, Smith SB, Spencer TE, Fried SK, Wu G, Dietary L-arginine supplementation reduces white fat gain and enhances skeletal muscle and brown fat masses in diet-induced obese rats. J. Nutr 139, 230–237 (2009). [PubMed: 19106310]

53. Carlstrom M, Larsen FJ, Nystrom T, Hezel M, Borniquel S, Weitzberg E, Lundberg JO, Dietary inorganic nitrate reverses features of metabolic syndrome in endothelial nitric oxide synthase-deficient mice. Proc. Natl. Acad. Sci. U. S. A 107, 17716–17720 (2010). [PubMed: 20876122]

54. Roberts LD, Ashmore T, Kotwica AO, Murfitt SA, Fernandez BO, Feelisch M, Murray AJ, Griffin JL, Inorganic nitrate promotes the browning of white adipose tissue through the nitrate-nitrite-nitric oxide pathway. Diabetes 64, 471–484 (2015). [PubMed: 25249574]

55. De Palma C, Falcone S, Pisoni S, Cipolat S, Panzeri C, Pambianco S, Pisconti A, Allevi R, Bassi MT, Cossu G, Pozzan T, Moncada S, Scorrano L, Brunelli S, Clementi E, Nitric oxide inhibition of Drp1-mediated mitochondrial fission is critical for myogenic differentiation. Cell Death Differ. 17, 1684–1696 (2010). [PubMed: 20467441]

56. Kikuchi-Utsumi K, Gao B, Ohinata H, Hashimoto M, Yamamoto N, Kuroshima A, Enhanced gene expression of endothelial nitric oxide synthase in brown adipose tissue during cold exposure. Am. J. Physiol. Regul. Integr. Comp. Physiol 282, R623–626 (2002). [PubMed: 11792674]

57. Lu X, Solmonson A, Lodi A, Nowinski SM, Sentandreu E, Riley CL, Mills EM, Tiziani S, The early metabolomic response of adipose tissue during acute cold exposure in mice. Sci Rep 7, 3455 (2017). [PubMed: 28615704]

58. Hoffmann LS, Etzrodt J, Willkomm L, Sanyal A, Scheja L, Fischer AW, Stasch JP, Bloch W, Friebe A, Heeren J, Pfeifer A, Stimulation of soluble guanylyl cyclase protects against obesity by recruiting brown adipose tissue. Nat. Commun 6, 7235 (2015). [PubMed: 26011238]

59. Vijgen GH, Sparks LM, Bouvy ND, Schaart G, Hoeks J, van Marken Lichtenbelt WD, Schrauwen P, Increased oxygen consumption in human adipose tissue from the "brown adipose tissue" region. J. Clin. Endocrinol. Metab 98, E1230–1234 (2013). [PubMed: 23783102]

60. van der Lans AA, Hoeks J, Brans B, Vijgen GH, Visser MG, Vosselman MJ, Hansen J, Jorgensen JA, Wu J, Mottaghy FM, Schrauwen P, van Marken Lichtenbelt WD, Cold acclimation recruits human brown fat and increases nonshivering thermogenesis. J. Clin. Invest 123, 3395–3403 (2013). [PubMed: 23867626]

61. Cypess AM, Weiner LS, Roberts-Toler C, Franquet Elia E, Kessler SH, Kahn PA, English J, Chatman K, Trauger SA, Doria A, Kolodny GM, Activation of human brown adipose tissue by a beta3-adrenergic receptor agonist. Cell Metab. 21, 33–38 (2015). [PubMed: 25565203]

62. Trayhurn P, Brown Adipose Tissue-A Therapeutic Target in Obesity? Front. Physiol 9, 1672 (2018). [PubMed: 30532712]

63. Eisner V, Cupo RR, Gao E, Csordas G, Slovinsky WS, Paillard M, Cheng L, Ibetti J, Chen SR, Chuprun JK, Hoek JB, Koch WJ, Hajnoczky G, Mitochondrial fusion dynamics is robust in the heart and depends on calcium oscillations and contractile activity. Proc. Natl. Acad. Sci. U. S. A 114, E859–E868 (2017). [PubMed: 28096338]

64. Wang CH, Chen YF, Wu CY, Wu PC, Huang YL, Kao CH, Lin CH, Kao LS, Tsai TF, Wei YH, Cisd2 modulates the differentiation and functioning of adipocytes by regulating intracellular Ca2+ homeostasis. Hum. Mol. Genet 23, 4770–4785 (2014). [PubMed: 24833725]

65. Rockl KS, Hirshman MF, Brandauer J, Fujii N, Witters LA, Goodyear LJ, Skeletal muscle adaptation to exercise training: AMP-activated protein kinase mediates muscle fiber type shift. Diabetes 56, 2062–2069 (2007). [PubMed: 17513699]

66. Gravel SP, Andrzejewski S, Avizonis D, St-Pierre J, Stable isotope tracer analysis in isolated mitochondria from mammalian systems. Metabolites 4, 166–183 (2014). [PubMed: 24957021]

67. Jaffrey SR, Snyder SH, The biotin switch method for the detection of S-nitrosylated proteins. Sci. STKE 2001, pl1 (2001).

68. Chouchani ET, Methner C, Nadtochiy SM, Logan A, Pell VR, Ding S, James AM, Cocheme HM, Reinhold J, Lilley KS, Partridge L, Fearnley IM, Robinson AJ, Hartley RC, Smith RA, Krieg T, Brookes PS, Murphy MP, Cardioprotection by S-nitrosation of a cysteine switch on mitochondrial complex I. Nat. Med 19, 753–759 (2013). [PubMed: 23708290]
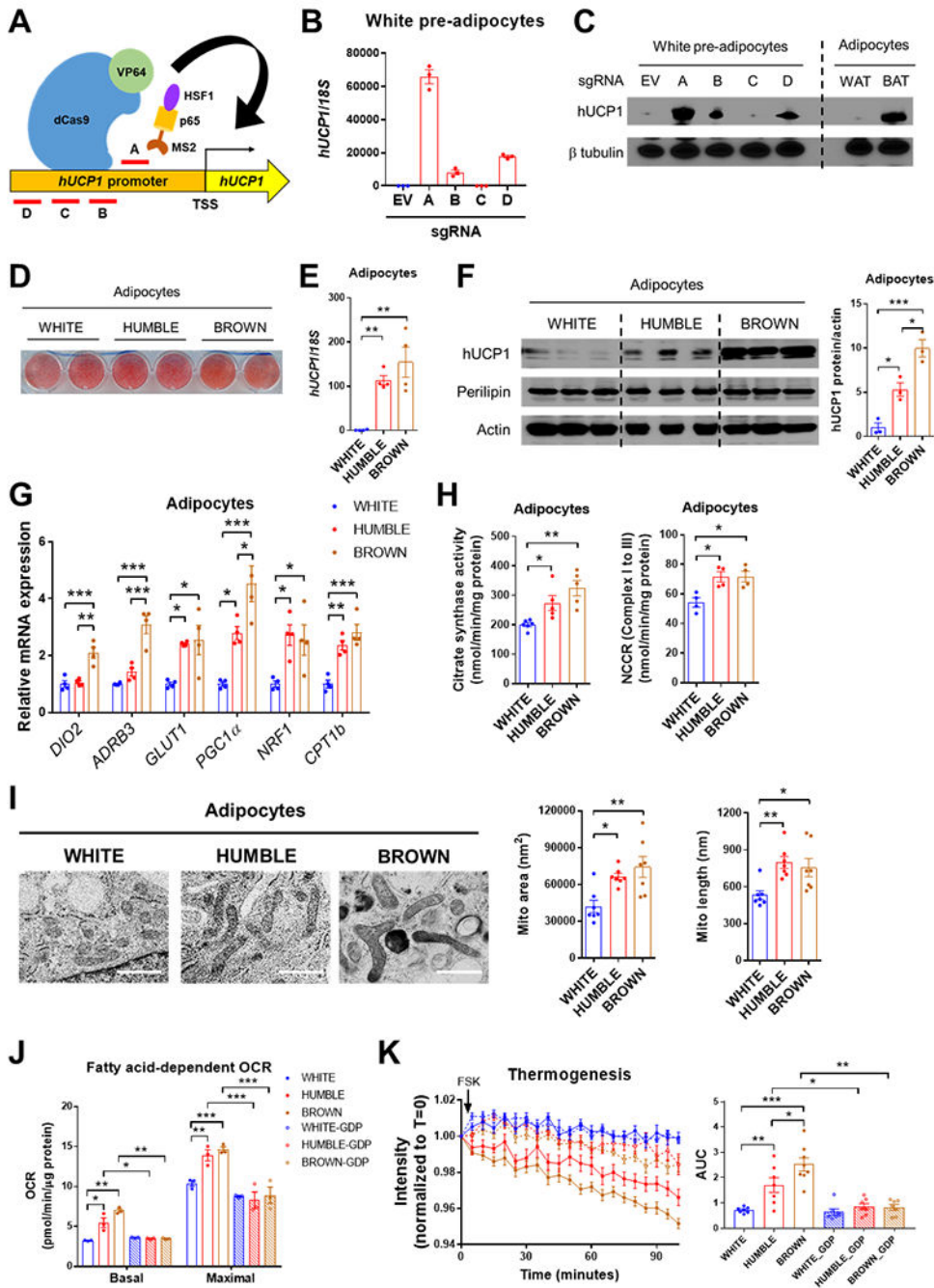
**Fig. 1. Activation of endogenous UCP1 by CRISPR-SAM triggers brown-like phenotypes in human white adipocytes.**

(A) Schematic positions of 4 different sgRNAs (labelled A-D) for targeting the human *UCP1* promoter with the CRISPR-SAM system. (B) *UCP1* mRNA expression in human white preadipocytes transfected with the CRISPR-SAM system and either empty vector (EV) or 4 different sgRNAs (A-D); n = 3 biological replicates per group. (C) UCP1 protein expression in white preadipocytes with EV or sgRNAs A-D compared with mature adipocytes differentiated from human white (WAT) and brown (BAT) preadipocytes. A representative immunoblot from 3 replicate experiments is presented. (D) Oil red O staining

in differentiated adipocytes from white preadipocytes transfected with EV (white control) or sgRNA-A (HUMBLE) and brown preadipocytes (brown control). (E) *UCP1* mRNA expression in white control, HUMBLE and brown control adipocytes; n = 4 biological replicates per group. (F) UCP1 protein expression in white control, HUMBLE and brown control adipocytes. A representative immunoblot and quantification of the mean from 3 replicate experiments is presented. (G) mRNA expression of key thermogenic genes in differentiated white control, HUMBLE, and brown control adipocytes; n = 4 biological replicates per group. (H) Citrate synthase activity (n=5 per group) and mitochondrial NADH cytochrome c reductase activity (NCCR, Complex I to III; n=4 per group) in total protein extracted from differentiated white control, HUMBLE, and brown control adipocytes. (I) Mitochondrial morphology and quantification of mitochondrial area and length in differentiated white control, HUMBLE, and brown control adipocytes using high-pressure freezing with transmission electronic microscopy (HPF-TEM). Data presented are representative micrographs with 1 μm scale bars and quantification of mitochondrial area and length in 7 individual cells per group (~30 mitochondria per cell). (J) Fatty acid-dependent OCR in differentiated white control, HUMBLE and brown control adipocytes treated with vehicle or 1 mM GDP; N = 3 technical replicates per group. (K) ERthermAC dye intensity in response to forskolin (FSK) treatment in differentiated white control, HUMBLE and brown control adipocytes treated with vehicle or 1 mM GDP; N = 8 technical replicates per group. For all graphs, data are presented as means ± s.e.m.; $*p < 0.05$; $**p < 0.01$; $***p < 0.001$.
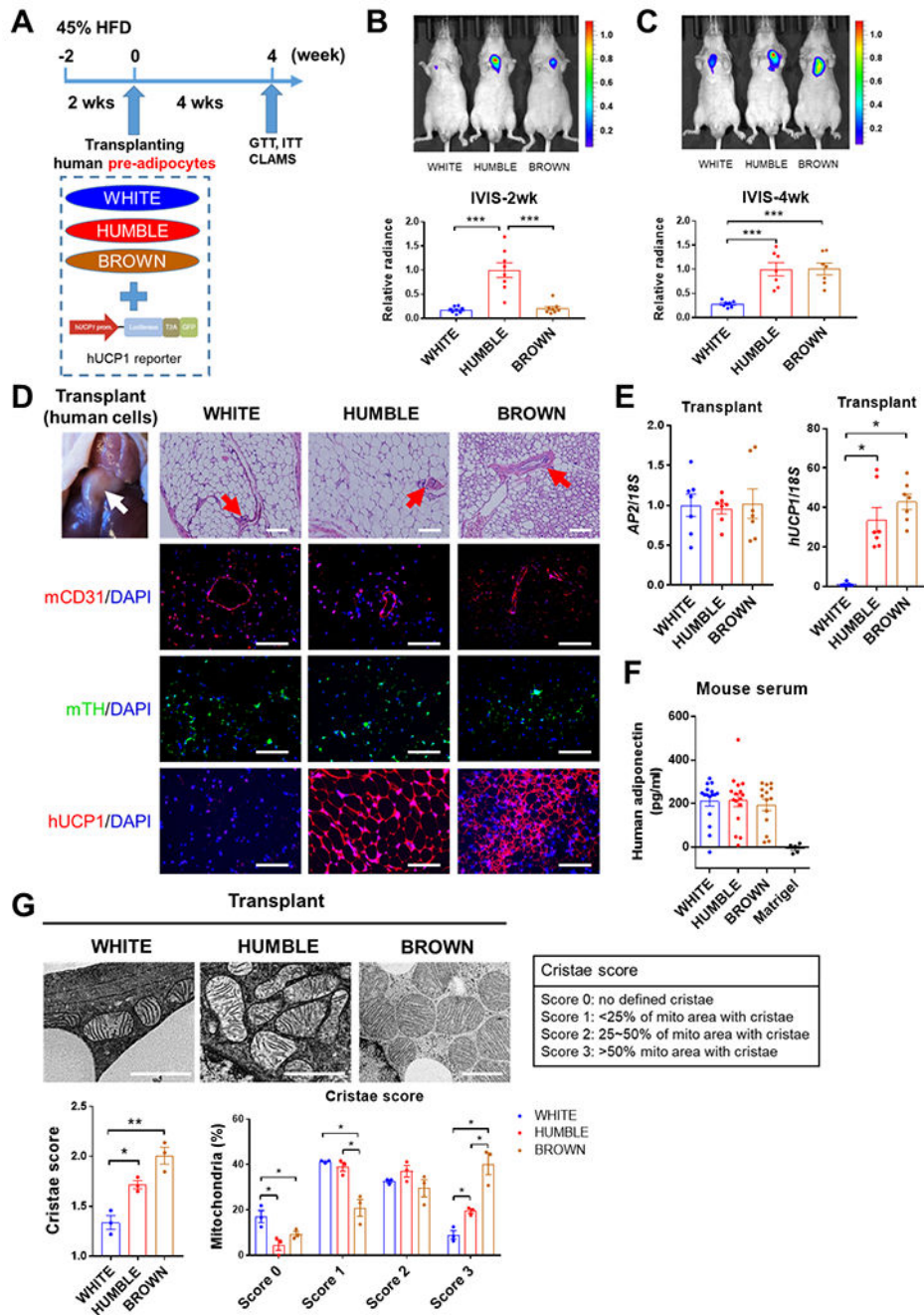
**Fig. 2. Transplanted white control, HUMBLE, or brown control cells reconstitute functional adipose tissue in mice.**

(A) Protocol schematic for transplantation of white control, HUMBLE, and brown control preadipocytes into nude mice. After mice were fed with 45% HFD for 2 weeks, cells transduced with a *UCP1* reporter construct were transplanted into thoracic-sternum region and mice were fed with 45% HFD for a further 4 weeks before a glucose tolerance test (GTT), insulin tolerance test (ITT), and metabolic analysis with the Comprehensive Lab Animal Monitoring System (CLAMS). (B and C) *UCP1* promoter activity measured by in vivo bioluminescence imaging in mice 2 weeks (B) and 4 weeks (C) after transplantation
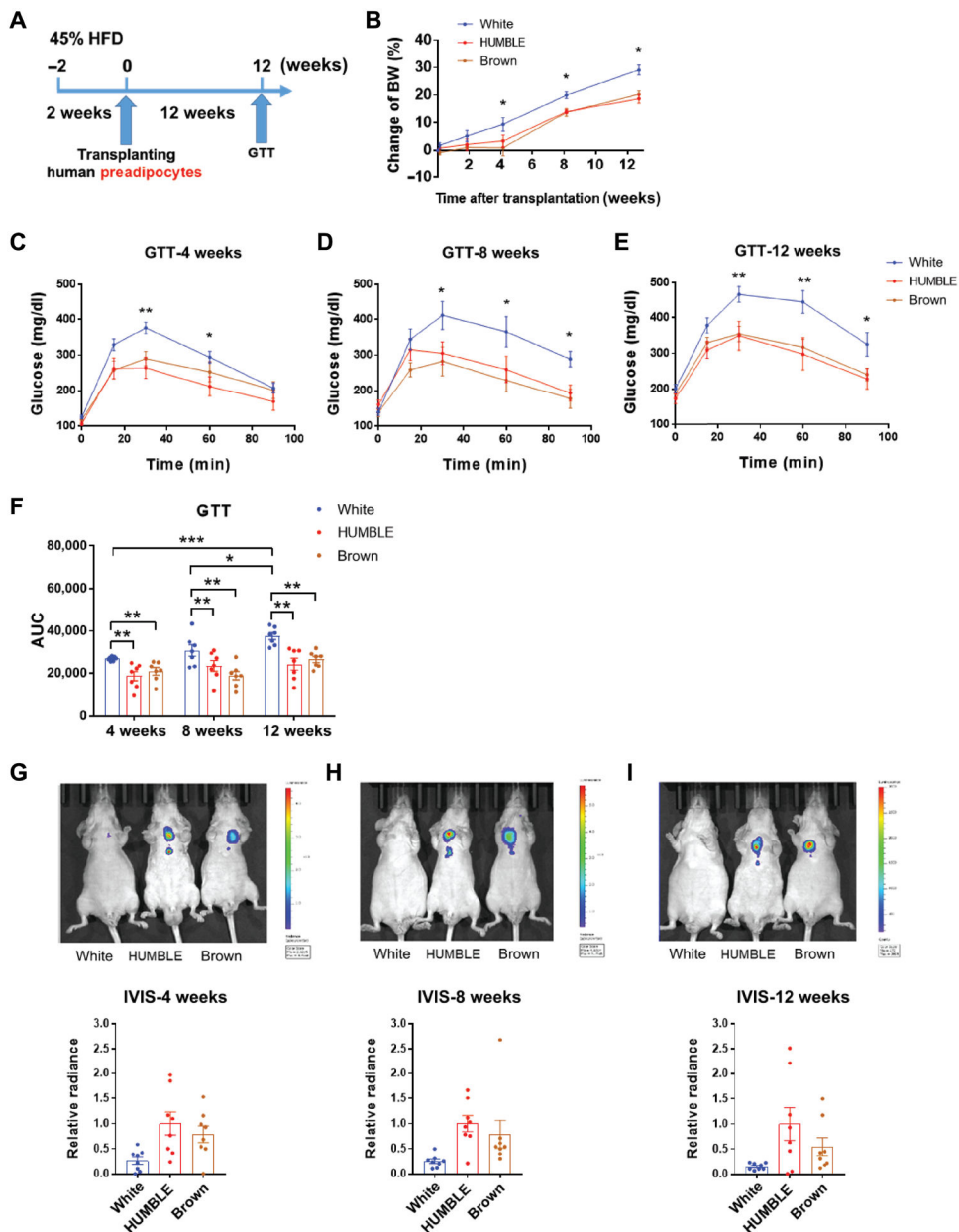
with white control, HUMBLE, or brown control cells. A representative image of n=8 experimental animals per group (upper) and quantification of luminescence (bottom) are shown. (D) H&E staining and immunostaining of human cell transplants after dissection from mice 4 weeks after transplantation with either white control, HUMBLE, or brown control cells. Sections were stained for mouse CD31 (mCD31), mouse tyrosine hydroxylase (mTH), and human UCP1 (hUCP1). The white arrow indicates the transplanted fat-like human tissue and the red arrows indicate vascular structures. Representative micrographs with 100 μm scale bars are shown; n = 8 mice per group. (E) Human specific *AP2* and *UCP1* mRNA expression measured by qPCR in transplanted tissues dissected from mice 4 weeks after receiving white control, HUMBLE, or brown control cells; n = 4 mice per group. (F) Human adiponectin relative abundance in serum of mice 4 weeks after transplantation with Matrigel only or with white control, HUMBLE or brown control cells; n = 5 mice with Matrigel, n=15 mice per cell transplant group. (G) Mitochondrial morphology in transplants assessed by HPF-TEM 4 weeks after transplantation of white control, HUMBLE, and brown control cell. Data are presented as representative micrographs with 1 μm scale bars (left). Mitochondrial cristae in the transplants were assessed based on different criteria (right). Mean cristae scores and percentage of mitochondria with different cristae scores in white control, HUMBLE, and brown control transplants were quantified. For all graphs, data are presented as means ± s.e.m.; *p < 0.05; **p < 0.01; ***p < 0.001.
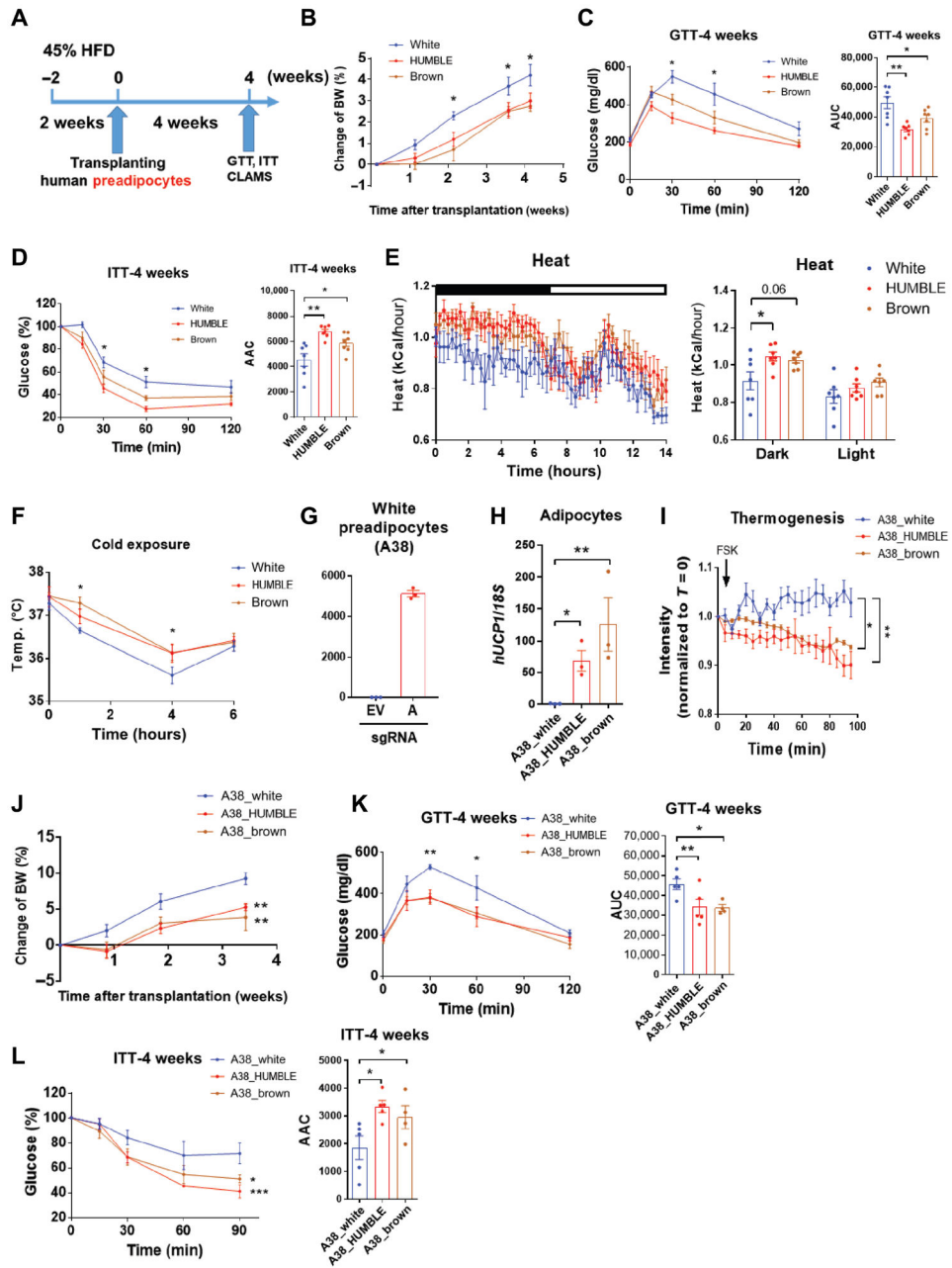
**Fig. 3. Transplantation of HUMBLE or brown control cells facilitates glucose metabolism and thermogenesis in mice.**

(A) Schematic protocol for transplantation of white control, HUMBLE or brown control preadipocytes into nude mice fed with 45% HFD. (B-D) Body weight (BW) change (B), GTT (C), and ITT (D) over 4 weeks in mice transplanted with white control, HUMBLE or brown control cells; n = 7 mice per group. (E) Heat production of mice 4 weeks after transplantation with white control, HUMBLE or brown control cells. Mean heat production over a 14-hour dark/light cycle (shown as the black/white bar above the left chart) was calculated (right); n = 7 mice per group. (F) Core body temperature of mice 4 weeks after transplantation with white control, HUMBLE, or brown control cells that were challenged at

5°C for 6 hours; n = 7 mice per group. (G) Human white preadipocytes from a second human subject (A38) were transfected with the CRISPR-SAM system and either empty vector (EV) or sgRNA-A and *UCP1* mRNA expression determined. (H and I) *UCP1* mRNA expression (H) and thermogenesis (I) in differentiated adipocytes from human A38 white preadipocytes transfected with EV (A38_white control) or sgRNA-A (A38_HUMBLE) and human brown A38 preadipocytes (A38_brown control). (J to L), BW change (J), GTT (K) and ITT (L) in mice over 4 weeks after transplantation with A38_white control, A38_HUMBLE or A38_brown control preadipocytes; n = 4 mice per group. In all charts, data are presented as means ± s.e.m.; *p < 0.05; **p < 0.01; ***p < 0.001.

**Fig. 4. HUMBLE cell transplantation results in long-term metabolic benefits in mice.**
(A) Schematic protocol for long-term transplantation of white control, HUMBLE or brown control preadipocytes into nude mice. (B) Body weight (BW) change in mice over 12 weeks after transplantation with white control, HUMBLE or brown control cells; n = 8 mice per group. (C to E) GTT in mice 4 weeks (C), 8 weeks (D), and 12 weeks (E) after transplantation with white control, HUMBLE or brown control cells; n = 8 mice per group. (F) Quantification of area under curve (AUC) in GTT after 4, 8, or 12 weeks of transplantation. (G to I) Representative images (upper) and quantification (lower) of *UCP1* luciferase reporter activity by IVIS in mice transplanted with white control, HUMBLE, or brown control 4 weeks (G), 8 weeks (H) and 12 weeks (I) after transplantation; n = 8 mice
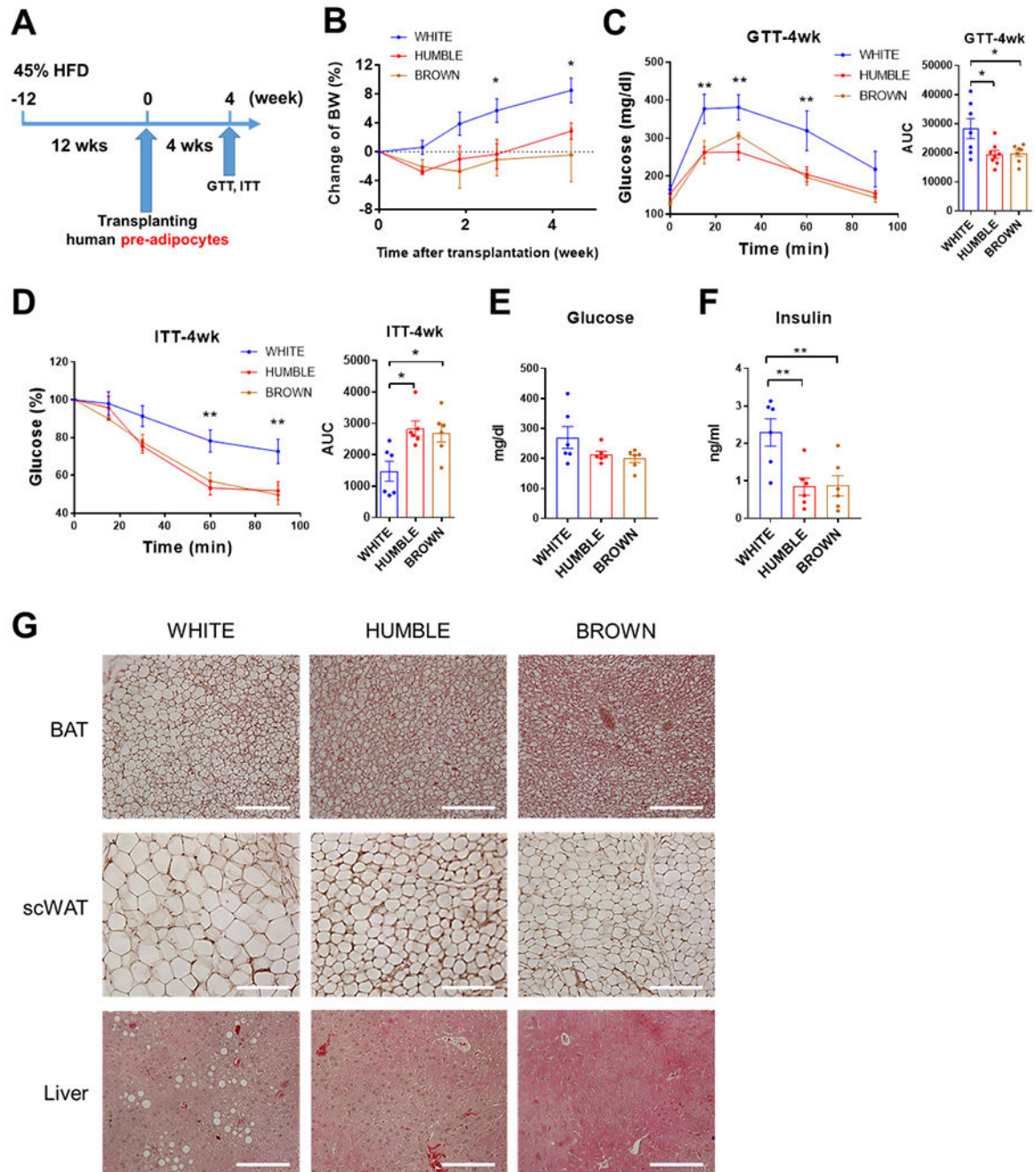
per group. In all charts, data are presented as means ± s.e.m.; *p < 0.05; **p < 0.01; ***p < 0.001.

**Fig. 5. HUMBLE cell transplantation improves metabolism in diet-induced obese mice.**
(A) Schematic protocol for transplantation of white control, HUMBLE and brown control preadipocytes into diet-induced obese (DIO) nude mice. (B) BW change over 4 weeks in DIO mice after transplantation with white control, HUMBLE or brown control preadipocytes; n = 6 mice per group. (C and D) GTT (C) and ITT (D) in DIO mice 4 weeks after transplantation with white control, HUMBLE or brown control cells; n = 6 mice per group. (E and F) Serum glucose (E) and insulin (F) concentration in DIO mice 4 weeks after transplantation with white control, HUMBLE or brown control preadipocytes; n = 6 mice per group. (G) H&E staining of BAT (upper), subcutaneous WAT (scWAT; middle), and liver
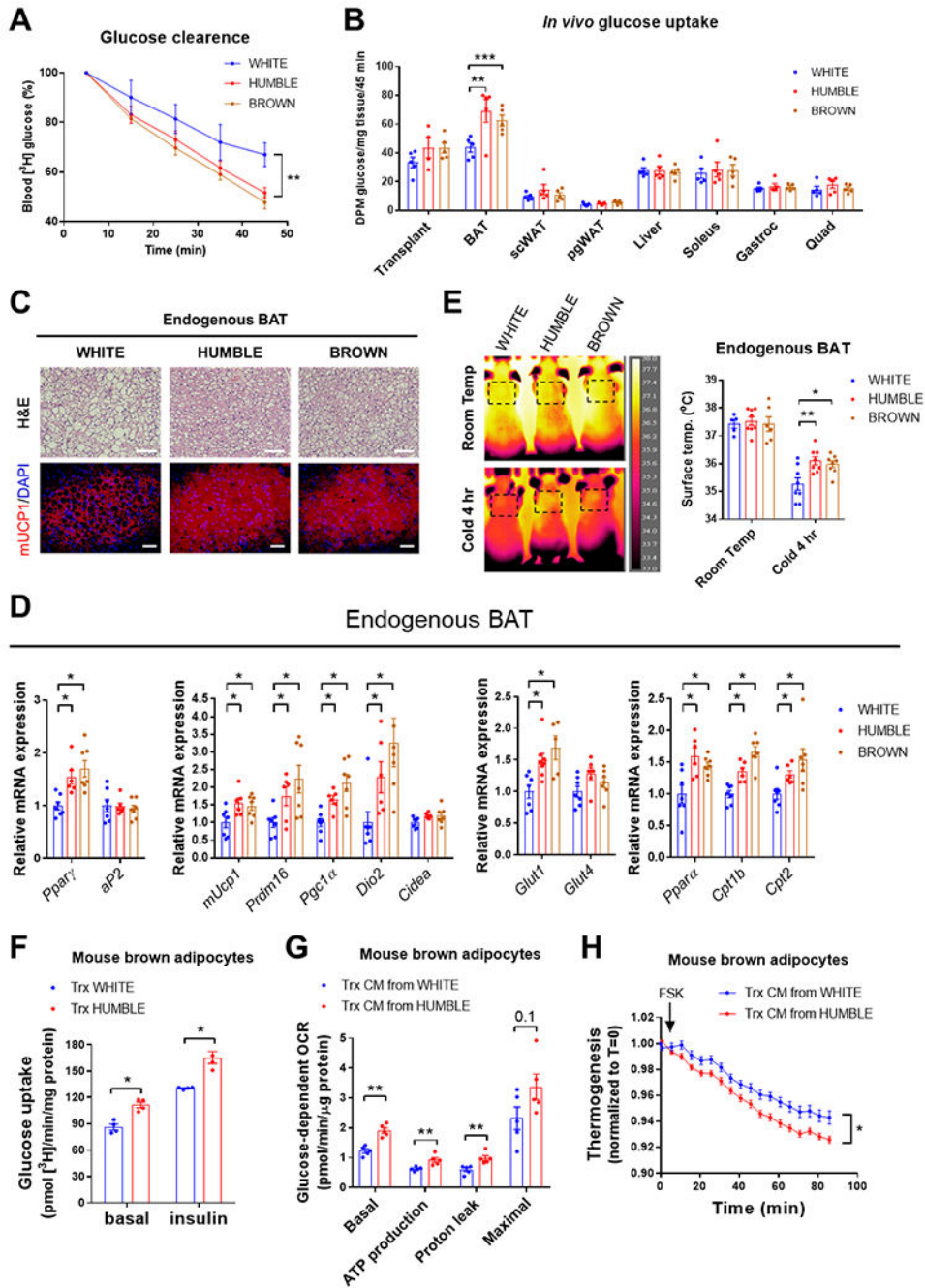
(lower) from DIO mice 4 weeks after transplantation with white control, HUMBLE, or brown control preadipocytes. Data are shown as representative micrographs with 100 μm scale bars. In all charts, data are presented as means ± s.e.m.; *p < 0.05; **p < 0.01.

**Fig. 6. HUMBLE cells activate endogenous murine BAT.**
(A) Radiolabeled [3H]-2-deoxyglucose clearance from circulation during 45 minutes after intravenous injection into mice 4 weeks after transplantation with white control, HUMBLE, or brown control cells; n = 6 mice per group. (B) Radiolabeled [3H]-2-deoxyglucose from different tissues 45 minutes after intravenous injection into mice 8 weeks after transplantation with white control, HUMBLE or brown control cells; n = 5 mice per group. (C) H&E staining (upper) and immunostaining for mouse UCP1 (mUCP1) in endogenous murine BAT from mice 4 weeks after transplantation with white control, HUMBLE or

brown control cells. Data are representative images with 100 μm scale bars from n=6 mice per group. (D) Endogenous murine BAT mRNA expression measured by qPCR from mice 4 weeks after transplantation with white control, HUMBLE or brown control cells; n = 6 mice per group. (E) Thermography of surface temperature of endogenous murine BAT in mice 4 weeks after transplantation with white control, HUMBLE or brown control cells. Data are representative images and quantification of n=5 mice per group before and after a 4-hr cold exposure at 5°C. (F) Glucose uptake in mouse brown adipocytes after 24-hr co-culture with white control or HUMBLE adipocytes; N = 4 technical replicates per group. (G) Glucose-dependent OCR measured by Seahorse in mouse brown adipocytes after 24-hr treatment with conditioned medium (CM) from white control or HUMBLE adipocytes; N = 5 technical replicates per group. (H) ERthermoAC dye intensity in response to forskolin (FSK) treatment in mouse brown adipocytes after 24-hr treatment with conditioned medium from white control or HUMBLE adipocytes; N = 12 technical replicates per group. For all charts, data are presented as means ± s.e.m.; $*p < 0.05$; $**p < 0.01$; $***p < 0.001$.
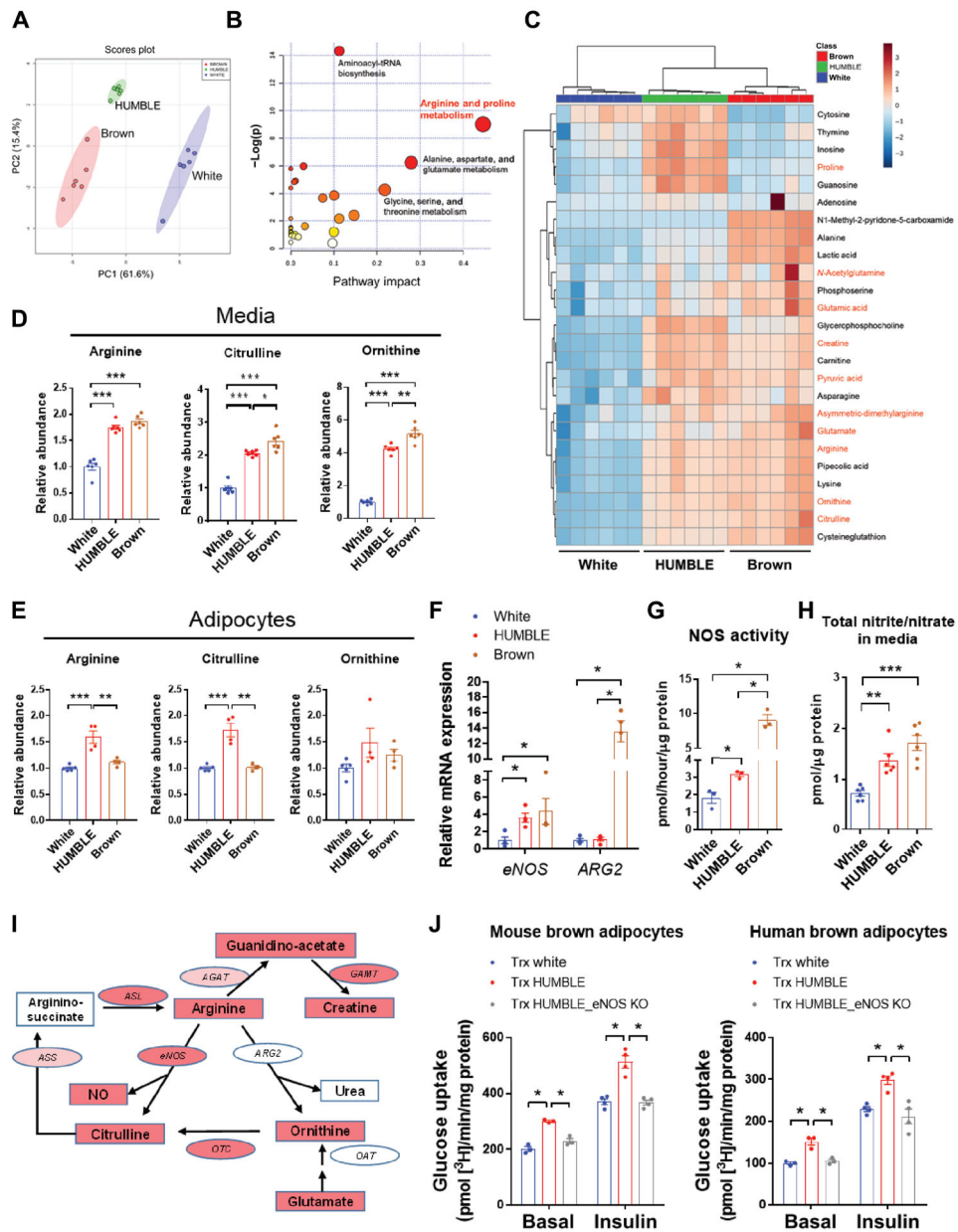
**Fig. 7. HUMBLE cells display elevated arginine and NO metabolism.**
(A to C) Principal component analysis (PCA) plot (A), pathway enrichment (B), and clustered heatmap (C) from metabolomics analysis of secreted media from differentiated white control, HUMBLE, or brown control adipocytes. Pathway impact in (B) indicates the degree centrality of changed metabolites in the pathway. Metabolites in (C) in red text are involved in arginine and proline metabolism; N = 6 technical replicates per group. (D and E) Relative abundance of arginine, citrulline, and ornithine in secreted media (D) and cell lysates (E) of differentiated white control, HUMBLE, or brown control adipocytes; N = 6 replicates per group for medium, N=4 replicates per group for lysate. (F) *eNOS* and *ARG2* mRNA expression were measured by qPCR in white control, HUMBLE, and brown control adipocytes; n = 4 biological replicates per group. (G and H) Total NOS activity (G) and total

nitric oxide concentration (nitrite and nitrate) in the medium (H) from differentiated white control, HUMBLE, and brown control adipocytes; n = 3 biological replicates per group for NOS activity, 5 biological replicates per group for total nitric oxide concentration. (I) Schematic of arginine metabolism pathway showing genes and metabolites differentially regulated in in vitro differentiated HUMBLE adipocytes compared to white control adipocytes. Strong (red) or slight (pink) increase of genes and metabolites in HUMBLE adipocytes compared to white control adipocytes. *NOS*, nitric oxide synthase; *ARG*, arginase; *OTC*, ornithine transcarbamylase; *OAT*, ornithine aminotransferase; *ASS*, argininosuccinate synthase; *ASL*, argininosuccinate lyase; *AGAT*, arginine:glycine amidinotransferase; *GAMT*, guanidinoacetate N-methyltransferase. (J) Glucose uptake in mouse (left) and human (right) brown adipocytes after 24-hr co-culture with white control, HUMBLE, and HUMBLE adipocytes with *eNOS* KO; N = 3 technical replicates per group. For all charts data are presented as means ± s.e.m.; *p < 0.05; **p < 0.01; ***p < 0.001.
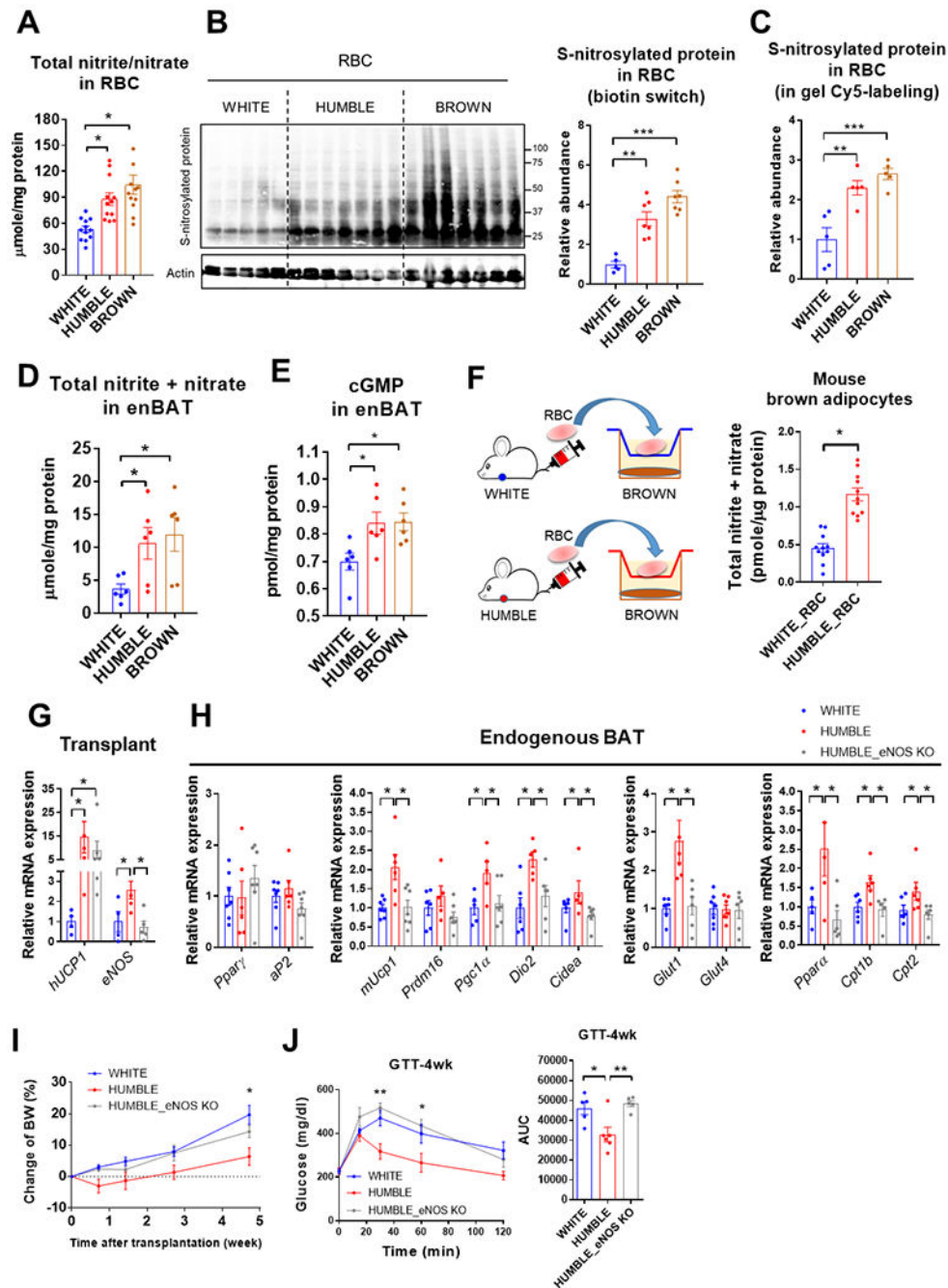
**Fig. 8. HUMBLE cells activate endogenous murine BAT via NO delivery by RBCs.**
(A) Total nitrite and nitrate concentration in RBCs from the mice 4 weeks after transplantation with white control, HUMBLE, or brown control cells; n = 12 mice per group for RBCs. (B and C) S-nitrosylated protein abundance in RBCs from the mice 4 weeks after transplantation with white control, HUMBLE or brown control cells detected by biotin switch (B) and gel Cy5-labeling (C); S-nitrosylated proteins were normalized by actin abundance in B or total protein in C. n = 5-7 mice per group. (D and E) Total nitrite and nitrate (D) and cGMP concentrations (E) in endogenous murine BAT (enBAT) from mice 4

weeks after transplantation with white control, HUMBLE, or brown control cells; n = 5-6 mice per group. (F) Schematic protocol for co-culture of mouse brown adipocytes with RBCs isolated from mice 4 weeks after transplantation with white control or HUMBLE preadipocytes (left panel). Total nitrite and nitrate concentrations (right panel) in mouse brown adipocytes after 4-hr co-culture with RBCs; n = 11 mice per group. (G) mRNA expression of *UCP1* and *eNOS* in transplanted tissues dissected from mice 4 weeks after transplantation with either white control, HUMBLE, or HUMBLE cells with *eNOS* KO; n = 4 mice per group. (H) mRNA expression of key adipogenic and thermogenic genes in endogenous murine BAT from mice 4 weeks after transplantation with either white control, HUMBLE, or HUMBLE cells with *eNOS* KO; n = 7 mice per group. (I and J) Body weight (BW) change (I) and GTT (J) of mice 4 weeks after transplantation with wild type HUMBLE cells, *eNOS* knockout HUMBLE cells (KO) or white control cells; n = 5 mice per group. For all charts, data are presented as means ± s.e.m.; *p < 0.05; **p < 0.01; ***p < 0.001.